

*Full Length Research Paper*

# Application of central composite design for preparation of Kenaf fiber based activated carbon for adsorption of manganese (II) ion

Z. Z. Chowdhury<sup>1\*</sup>, S. M. Zain<sup>1</sup>, R. A. Khan<sup>1</sup>, A. A. Ahmad<sup>2</sup>, M. S. Islam<sup>3</sup> and Arash Arami-Niya<sup>3</sup>

<sup>1</sup>Department of Chemistry, Faculty of Science, University Malaya, Kuala Lumpur 50603, Malaysia.

<sup>2</sup>Department of Chemical and Environmental Engineering, Faculty of Engineering, University Putra Malaysia, 43400 UPM, Serdang, Malaysia.

<sup>3</sup>Department of Chemical Engineering, Faculty of Engineering, University Malaya, Kuala Lumpur 50603, Malaysia.

Accepted 18 October, 2011

The objective of this research is to define optimum operating conditions for preparation of activated carbon from kenaf fiber which would conciliate for highest removal efficiency of manganese (II) ions along with maximum possible yield. Kenaf fiber (KF) is used to prepare activated carbon by using two step; physiochemical activation method which consisted of potassium hydroxide treatment (KOH) with carbon dioxide gasification. The effects of three preparation variables; temperature (500 to 700°C), time (1 to 3 h) and KOH impregnation ratio, IR (1-3) on the percentage yield and removal percentage of Mn (II) ions were investigated. Based on central composite design (CCD), quadratic models were developed to correlate activated carbon preparation variables with the aforementioned two responses. From the analysis of variance (ANOVA), the most influential factor on each experimental design response was identified. The optimum conditions determined were: activation temperature, activation time and impregnation ratio, IR of 574°C, 1.31 h and 3, respectively. The application of prepared activated carbon under optimum condition was further analyzed by Langmuir, Freundlich and Temkin isotherm. The values of Langmuir separation factor,  $R_L$  and Freundlich exponent,  $1/n$  were less than 1 reflecting favorable process for adsorption.

**Key words:** Kenaf fiber, activated carbon, adsorption, manganese Mn (II), optimization, central composite design, analysis of variance (ANOVA), response surface methodology.

## INTRODUCTION

The adsorption process is being widely used by many researchers for the removal of inorganic and organic pollutants from contaminated streams. Commercially available activated carbon has been frequently employed for thousands of years in many adsorption processes for removal of impurities from liquids and gases (Mattson and Merck, 1971). It contains lot of graphite like microcrystalline unit linked together, similar to that of carbon black (Do, 1996). The effectiveness of activated carbon as an adsorbent attributed to its unique properties including highly developed internal surface area between

500 and 2000 m<sup>2</sup>/g, favorable pore size and high degree of surface reactivity due to presence of surface functional groups, especially oxygen groups (Ismadji and Bhatia, 2001). Their structure is complex and heterogeneous due to presence of micropores, mesopores and macro pores of different size and shape. Despite its extensive use in synthetic waste water treatment, commercial activated carbon remains an expensive material. Therefore, in recent years, the need for economical methods for elimination of toxic metals from contaminated water has necessitated research interest towards the production of activated carbon from inexpensive agro based waste material. However, the adsorption property of activated carbon is highly influenced by its preparation conditions. The preparation variables of temperature, time and impregnation ratio will significantly change its surface area,

\*Corresponding author. E-mail: [zairachowdhury76@gmail.com](mailto:zairachowdhury76@gmail.com)  
com. Tel: +60166685385. Fax: +60379674193/4444.

**Table 1.** List of agro-based by products used for preparation of activated carbon.

<b>Agricultural by product</b>	<b>Reference</b>
Coconut shell	Hu and Srinivasan (1999)
Coffee bean husk	Baquero et al. (2003)
Oil palm fiber	Hameed et al. (2008)
Rubber wood saw dust	Srinivasakannan and Bakar (2004)
Chest nut wood	Gomez-Serrano et al. (2005)
Fruit Stone	Puziy et al. (2005)
Bamboo waste	Ahmad and Hameed (2010)
Grain sorghum	Diao et al. (2002)
Rattan sawdust	Ahmad et al. (2009)
Cassava Peel	Sudaryanto et al. (2006)
Oil Seed waste	Stavropoulos and Zabaniotou (2005)

pore size distribution and surface functional groups. Therefore, it is a challenge to produce specific types of activated carbon which are suitable for certain applications. Petroleum residues like coal, lignite, peat and wood which are rich in carbon are commonly used precursors for production of commercial activated carbon. However, production of activated carbon from these non renewable starting materials makes it expensive. This is the reason, the use of low cost agricultural waste either by chemical activation or by producing activated carbon is considered as a better choice (Egila et al., 2011; Prahas et al., 2008). Following Table 1 depicts that until recently, many agricultural by-products have been successfully used to produce activated carbon due to their high carbon and low ash content.

The objective of this research was to explore the feasibility of producing activated carbon from kenaf by using response surface methodology (RSM). Renewable starting materials like Kenaf have been chosen as adsorbate to prepare activated carbon is due to its abundant availability in nature. Recently, the Government of Malaysia has allocated around 12 million RM (Aber et al., 2009) for research and further development of the kenaf-based industry under the 9th Malaysia Plan (2006 to 2010). The removal efficiency of Mn (II) ions along with maximum possible yield can be increased by optimizing the operating factors. By using this technique, the interactions of possible influencing parameters on sorption efficiency can be evaluated and optimized with a limited number of planned experiments (Lee et al., 2000). RSM has been previously used for preparing activated carbon from olive waste cakes by physical activation (Stavropoulos and Zabaniotou, 2005), sewage sludge by chemical activation (Tay et al., 2001), Turkish lignite by chemical activation (Karakan et al., 2007), coconut shell (Gratuito et al., 2008), coconut husk (Tan et al., 2008) and hazel nut shell (Sayan, 2006). Unlike other organic waste and other heavy metals, Mn (II) is persistent in nature and it can reach up to the highest member of food chain causing potential risk for human health as well as

aquatic lives (Akpore and Muchie, 2010). According to Irving William Series, it is well known that, Mn (II) has got the least tendency to form stable surface complexes. Thus the removal of Mn (II) from contaminated water by adsorption technique is difficult. Intake of Mn (II) more than the tolerance limit can cause severe disorder in nervous system (Chowdhury et al., 2011a). Above perusal of the literature reflects that, no studies have been carried out on kenaf fiber based activated carbon to remove Mn (II) ions from contaminated water by using response surface methodology (RSM). A central composite design (CCD) was selected to study simultaneously the effects of three factors: temperature, activation time and impregnation ratio on the two responses: Carbon yield and percentage removal of Mn (II) from aqueous phase. Consequently, surface characterization of prepared activated carbon was analyzed in terms of BET surface analysis, Fourier transform infrared (FTIR) scanning electron microscopy (SEM) and elemental composition analysis. Furthermore, equilibrium isotherm model parameters were determined to have insight about the sorption phenomenon.

## MATERIALS AND METHODS

### Preparation of activated carbon

Kenaf fibers used in this work were supplied by MARDI (Malaysian Agricultural Research and Development Institute). The fibers were washed with hot distilled water and it was dried at 105° for 24 h to remove all moisture. The dried samples were cut into small pieces and were sieved to the size of 1 to 2 mm. For producing char, 40 g of dried fiber samples were placed on the metal mesh located at the bottom of the tubular reactor. The flow rate of purified nitrogen gas and the heating rate were kept constant at 150 and 10°C/min respectively. Semi carbonization was done at temperature 400°C and for 2 h. The char was allowed to cool down at room temperature under nitrogen flow and stored in air-tight containers. Depending on impregnation ratio, a specific amount of KOH pellets were mixed together with 40 g of char and 250 ml deionized water was added in a 500 ml beaker with occasional stirring to dissolve all

**Table 2.** Experimental factors in coded and actual units and experimental responses.

Run	Type	X <sub>1</sub> : Temperature code	X <sub>2</sub> : time. code	X <sub>3</sub> : IR. code	Temperature (°C)	Time (h)	IR	% yield (Y <sub>1</sub> )	% Removal of Mn(II) (Y <sub>2</sub> )
1	Center	0	0	0	600	2	2	18.98	89.9
2	Fact	-1	1	1	500	3	3	22.09	75.98
3	Axial	0	-1.682	0	600	0.32	2	26.78	70.07
4	Center	0	0	0	600	2	2	17.78	90
5	Fact	1	1	-1	700	3	1	14.99	78.99
6	Center	0	0	0	600	2	2	18.65	88.43
7	Fact	1	-1	-1	700	3	1	23.98	70.23
8	Center	0	0	0	600	2	2	17.99	87.89
9	Axial	0	0	1.682	600	2	3.68	13.99	91.09
10	Fact	1	1	1	700	3	3	5.77	90.95
11	Fact	-1	1	1	500	3	1	32.02	71.89
12	Fact	-1	-1	-1	500	1	1	33.89	70.76
13	Fact	1	-1	1	700	1	3	19.99	89.11
14	Fact	-1	-1	1	500	1	3	26.99	78.99
15	Center	0	0	0	600	2	2	19.88	88.1
16	Axial	0	1.682	0	600	3.68	2	14.88	74.78
17	Axial	1.682	0	0	768.18	2	2	9.98	82.89
18	Center	0	0	0	600	2	2	16.67	88.34
19	Axial	-1.682	0	0	431.82	2	2	34.99	70.99
20	Axial	0	0	-1.682	600	2	0.32	27.89	72.89

KOH pellets. Then the beaker was placed inside an oven overnight at temperature 105°C for dehydrating and leaving only KOH onto the sample. The impregnation ratio can be calculated by using Equation (1):

$$\text{Impregnation ratio (IR)} = \frac{W_{KOH}}{W_{Char}} \quad (1)$$

Here,  $W_{KOH}$  is the dry weight of potassium hydroxide pellets and  $W_{char}$  is the dry weight of char.

Exactly weighted amount of KOH impregnated chars were placed inside the tubular furnace with nitrogen gas flow rate of 150 cm<sup>3</sup>/min and heating rate of 10°C/min. The temperature was ramped from room temperature to desired activation temperature. Once desired activation temperature was reached, the gas flow was switched to carbon dioxide at the same flow rate and kept constant for certain duration of time. The prepared activated carbon was cooled to room temperature under nitrogen gas flow. Then the final product was washed with hot deionized water for several times to remove the remaining KOH. During the washing process, 0.1 M hydrochloric acid was used until the pH of the washing solution reached 6 to 7. The washed samples of activated carbon was dried at 105°C in an oven until it was completely dried and stored in air-tight container for further applications.

KOH has been chosen due to its high reactivity towards the cellulosic precursors in presence of physical activating agents of carbon dioxide. It acts as a strong dehydrating agent rather than other alkali and during the activation step it can exfoliate the carbon matrix at high temperature. It can form K<sub>2</sub>O which can react with CO<sub>2</sub> to produce K<sub>2</sub>CO<sub>3</sub> by water shift reaction (Salman and Hameed 2010; Tan et al. 2008). Basically, introduction of this metallic potassium in hydroxide form is the key factor for breakdown of

cellulosic chain and drastic expansion of surface area and pore volume of the prepared activated carbon from kenaf fiber.

### Design of Experiments (DOE)

The complete design matrix for 20 experimental designs together with the results obtained is shown in Table 2. According to central composite design, for each variable, a 2<sup>3</sup> full factorial CCD for the three variables consisting of eight factorial points, six axial points and six replicates at the center points were employed, representing that altogether 20 experiments should be carried out to find out the optimum preparation conditions, and can be calculated by Equation (2).

$$N = 2^n + 2n + nc = 2^3 + 2 \times 3 + 6 = 20 \quad (2)$$

where, N is the total number of experiments required and n denotes the number of factors.

The independent variables were coded to the (-1, 1) interval. The low and high levels were denoted by -1 and +1, respectively. The axial points were located at (0, 0, ±α), (0, ±α, 0) and (±α, 0, 0). Here, α was the distance of the axial point from center. The two responses of activated carbon yield (Y<sub>1</sub>) and removal % of Mn (II) ions (Y<sub>2</sub>) were determined. Table 3 summarizes the ranges and the levels of the variables studied here for preparing activated carbon. An empirical model was developed for each response which correlated the response with three preparation variables using a second degree polynomial equation (Zainuddin et al., 2005; Parajo et al., 1992) as can be given by following Equation (3):

$$Y = b_0 + \sum_{i=1}^n b_i x_i + \left( \sum_{i=1}^n b_{ii} x_i \right)^2 + \sum_{i=1}^{n-1} \sum_{j=i+1}^n b_{ij} x_i x_j \quad (3)$$

**Table 3.** Independent variables and their coded levels for the central composite design.

Variable	Code	Unit	Coded variable level				
			- $\alpha$	-1	0	+1	+ $\alpha$
Temperature	X <sub>1</sub>	°C	431.82	500	600	700	768.18
Activation time	X <sub>2</sub>	Hour	0.32	1	2	3	3.68
Impregnation ratio	X <sub>3</sub>	-	0.32	1	2	3	3.68

**Table 4.** Analysis of variances (ANOVA) and lack-of-fit test for response surface quadratic model for yield.

Value of R <sub>L</sub>	Types of isotherm
R <sub>L</sub> > 1	Unfavorable
R <sub>L</sub> = 1	Linear
0 < R <sub>L</sub> < 1	Favorable
R <sub>L</sub> = 0	Irreversible

Here,  $\gamma$  = the predicted response;  $b_0$  = the constant coefficient;  $b_i$  = the linear coefficients;  $b_{ij}$  = the interaction coefficients;  $b_{ii}$  = the quadratic coefficients respectively and  $x_i$ , and  $x_j$  = the coded values of the activated carbon preparation variables.

#### Model development and statistical analysis

The regression equations and graphical analysis for each response with statistical significance were performed by using Design-Expert software (version 6, Stat-Ease, Inc., Minneapolis, USA). In order to evaluate the relationship between the experimental variables and responses, the response surface and contour plots were generated.

#### Adsorption studies

Batch adsorption for prepared activated carbon in 20 run selected by the software was performed in 20 sets of 100 ml Erlenmeyer flasks where 50 ml of manganese chloride (MnCl<sub>2</sub>·2H<sub>2</sub>O) salt solution of initial Mn (II) ion concentration of 100 mg/L was added. The pH of the solution was adjusted to 5.5 to avoid preprecipitation. 0.20 g of each of the prepared activated carbon, with particle size of 200 to 300  $\mu$ m was added to each flask and kept in a thermostatic water bath shaker using 150 rpm at 30°C until equilibrium was reached. Aqueous samples were taken from the solutions at definite interval of time until equilibrium was reached. The remaining concentrations of Mn (II) ions in the solutions after adsorption were determined using an atomic absorption spectrophotometer (Perkin – Elmer Model 3100). However, for isotherm generation concentration range was varied from 50, 60, 70, 80, 90 and 100 mg/L. Fresh dilution of stock solution was carried out prior to each sorption study.

The amount of adsorption of Mn (II) ions at equilibrium,  $q_e$  (mg/g) was calculated by using the following Equation (4):

$$q_e = \frac{(C_0 - C_e)V}{W} \quad (4)$$

where,  $q_e$  (mg/g) is the amount of ion adsorbed at equilibrium;  $C_0$  and  $C_e$  (mg/L) are the liquid-phase concentrations of Mn (II) ions at

initial and equilibrium conditions, respectively;  $V$  (L) is the volume of the solution, and  $W$  (g) is the mass of activated carbon used. The linear form of Langmuir isotherm (Langmuir, 1916) equation is expressed by Equation (5):

$$\frac{C_e}{q_e} = \frac{1}{q_{\max} K_L} + \frac{C_e}{q_{\max}} \quad (5)$$

where,  $C_e$  (mg/L) is the equilibrium concentration of the adsorbate,  $q_e$  (mg/g) is the amount of adsorbate; Mn (II) ions, adsorbed per unit mass of adsorbent,  $q_{\max}$  (mg/g) is the maximum amount of the Mn (II) ions per unit weight of the activated carbon to form a complete monolayer on the surface where as  $K_L$  (l/mg) is Langmuir constant related to the affinity of the binding sites.

The essential characteristics of the Langmuir equation can be expressed in terms of a separation factor,  $R_L$  which is given as

$$R_L = \frac{1}{1 + K_L C_0} \quad (6)$$

$C_0$  is the highest initial cation concentration (mg/L). The values of separation factor  $R_L$ , can be summarized as shown in Table 4

The linear form of Freundlich (Freundlich 1906; Hefne et al., 2008) isotherm is

$$\ln q_e = \ln K_F + \frac{1}{n} \ln C_e \quad (7)$$

Here,  $K_F$  (mg/g) represents the affinity factor or multilayer adsorption capacity and  $1/n$  is the intensity of adsorption, respectively. According to Temkin Isotherm (Temkin and Pyzhev, 1940), the linear form can be expressed by Equation (8)

$$q_e = \frac{RT}{b} \ln K_T + \frac{RT}{b} \ln C_e \quad (8)$$

Here,  $RT/b = B$  (J/mol), which is Temkin constant related to heat of sorption, whereas  $K_T$  (l/g) represents the equilibrium binding constant corresponding to the maximum binding energy.  $R$  (8.314 J/mol K) is universal gas constant and  $T^\circ$  (K) is absolute solution temperature.

#### Activated carbon yield

The activated carbon yield was calculated based on Equation (9).

$$Yield \% = \frac{W_c}{W_0} \quad (9)$$

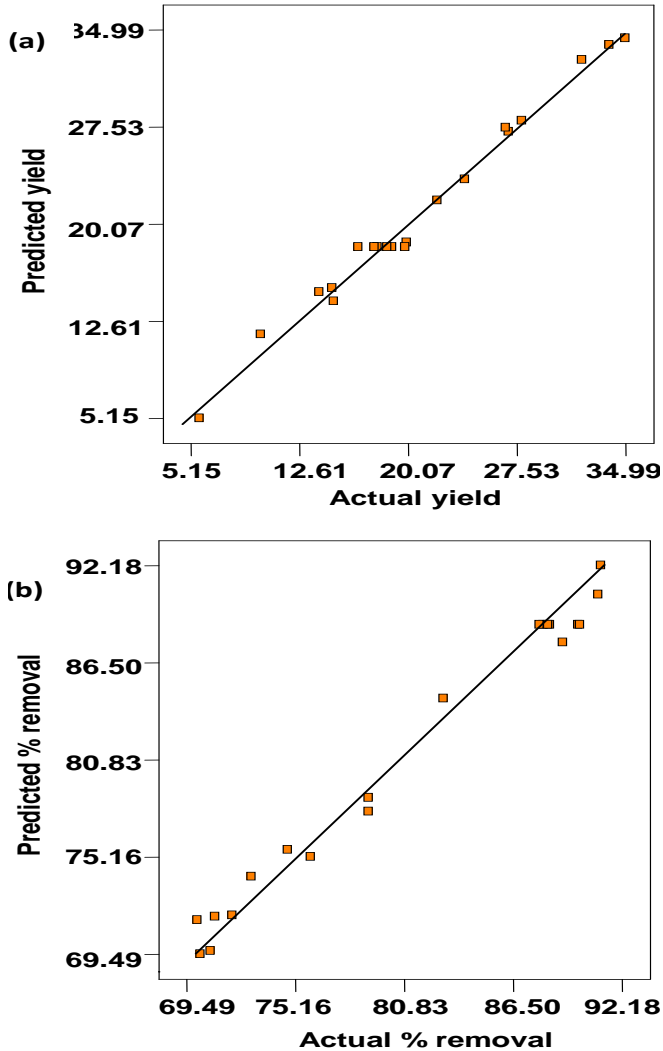


**Figure 1.** Predicted vs .actual data for (a) yield and (b) percentage removal.

where,  $W_c$  (g) is the dry weight of final activated carbon and  $W_0$  (g) is the dry weight of precursor.

#### Characterization of activated carbon

BET surface area, pore volume and pore diameter of the prepared adsorbent was measured by Autosorb1, Quantachrome Autosorb Automated gas sorption system supplied by Quantachrome. The average bulk density was determined by water displacement of a definite amount of activated carbon. The surface functional group of the prepared activated carbon was detected by Fourier Transform Infrared (FTIR) spectroscope (FTIR-2000, Perkin-Elmer). The spectra were recorded from 4000 to 400  $\text{cm}^{-1}$ .

Scanning electron microscopy (SEM) analysis was carried out on the precursor, semi carbonized precursor and the activated carbon (Leo Supra, Model 50VP Field Emission, UK). Elemental analysis was performed using Elemental Analyzer (PerkinElmer, Series II 2400) to investigate the presence of elements of carbon, hydrogen, and nitrogen in precursor and the activated carbon.

## RESULTS AND DISCUSSION

### Model development and statistical analysis

For both responses of percentage carbon yield and Mn (II) ions removal, the quadratic model was selected by the software. Multiple regression analysis was performed based on data obtained in Table 2 and used to correlate the responses with the three variables studied using a second order polynomial as shown by Equation (3). The quadratic regression models for yield ( $Y_1$ ) and removal percentage of Mn (II) ions ( $Y_2$ ) are given by Equations (10) and (11):

$$\begin{aligned} (\%) \text{ Carbon yield: } Y_1 = & 18.30 - 6.76X_1 - 3.66X_2 - 3.91X_3 - \\ & 1.65X_1^2 + 1.07X_2^2 - 1.11X_3^2 - 2.05X_1X_2 + 0.45X_1X_3 - \\ & 1.03X_2X_3 \end{aligned} \quad (10)$$

$$\begin{aligned} (\%) \text{ Percentage removal: } Y_2 = & 88.71 + 3.78X_1 + 1.22X_2 \\ & + 5.40X_3 - 3.77 X_1^2 - 5.37 X_2^2 - 1.99 X_3^2 - 1.56 X_1X_2 + \\ & 2.32 X_1X_3 - 1.32 X_2X_3 \end{aligned} \quad (11)$$

Here,  $X_1$ ,  $X_2$ , and  $X_3$  represents the coded values for temperature, time and impregnation ratio. Positive sign in front of the terms represents synergistic effect, whereas negative terms represent antagonistic effect. The coefficients with one factor of temperature, time and impregnation ratio represent the effect of that particular factor for the preparation of activated carbon. The coefficients with two factors and others with second order terms show the interaction between the two factors and quadratic effect respectively.

The quality of the model developed can be understood by correlation coefficient,  $R^2$  and standard deviation values.  $R^2$  indicates the ratio between sum of the squares (SSR) with total sum of the square (SST) and it depicts how well the model approximate experimental data points. The  $R^2$  values obtained here for percentage yield and percentage removal of Mn (II) ions are 0.987 and 0.985, respectively which ensures satisfactory adjustment of the quadratic model with the experimental data. The standard deviation obtained for yield and percentage removal was 1.19 and 1.35. The performance of the model can be also visualized by observing the plots of predicted versus experimental percentage yield and removal by Figure 1a and b.

The adequacy and significance of the model was justified through analysis of variance (ANOVA). The ANOVA for the quadratic model for yield is listed in Table 5. The model F- value for percentage yield observed was 88.51 revealing that the model was significant. Values of Prob> F less than 0.05 reflects that the model terms were significant. In this study,  $X_1$ ,  $X_2$ ,  $X_3$ ,  $X_1^2$ ,  $X_2^2$ ,  $X_3^2$ ,  $X_1X_2$  and  $X_2X_3$  were significant model terms.

Table 6 depicts the results of the second order response surface model fitting in the form of analysis of variance (ANOVA) for percentage removal of Mn (II) ions from synthetic waste water. The F- value of 77.53 implied

**Table 5.** Analysis of variances (ANOVA) and lack-of-fit test for response surface quadratic model for percentage removal of Mn (II).

Source of data	Sum of the square	Degree of freedom (DF)	Mean square	F value	Prob > F	Comment
Model	1122.05	9	124.67	88.51	< 0.0001	
X <sub>1</sub>	624.10	1	624.10	443.07	< 0.0001	
X <sub>2</sub>	183.01	1	183.01	129.29	< 0.0001	
X <sub>3</sub>	208.93	1	208.93	148.33	< 0.0001	
X <sub>1</sub> <sup>2</sup>	39.33	1	39.33	27.92	0.0004	
X <sub>2</sub> <sup>2</sup>	16.40	1	16.40	11.65	0.0066	Significant
X <sub>3</sub> <sup>2</sup>	17.62	1	17.62	12.51	0.0054	
X <sub>1</sub> X <sub>2</sub>	33.78	1	33.78	23.98	0.0006	
X <sub>2</sub> X <sub>3</sub>	8.53	1	8.53	6.05	0.0336	
X <sub>3</sub> X <sub>1</sub>	1.64	1	1.64	1.16	0.3062	
Residuals	14.09	10	1.41			
Lack-of -fit	7.98	5	1.60	1.31	0.3875	Not significant
Pure error	6.10	5	1.22			

**Table 6.** Analysis of variances (ANOVA) and lack-of-fit test for response surface quadratic model for percentage removal of Mn (II).

Source of data	Sum of the square	Degree of freedom (DF)	Mean square	F value	Prob> F	Comment
Model	1279.97	9	142.22	77.53	<0.0001	
X <sub>1</sub>	195.52	1	195.52	106.58	<0.0001	
X <sub>2</sub>	20.28	1	20.28	11.05	0.0077	
X <sub>3</sub>	398.47	1	398.47	217.22	<0.0001	
X <sub>1</sub> <sup>2</sup>	205.16	1	205.16	111.84	<0.0001	
X <sub>2</sub> <sup>2</sup>	415.48	1	415.48	226.50	<0.0001	Significant
X <sub>3</sub> <sup>2</sup>	56.94	1	56.94	31.04	0.0002	
X <sub>1</sub> X <sub>2</sub>	19.47	1	19.47	10.61	0.0086	
X <sub>2</sub> X <sub>3</sub>	15.29	1	15.29	8.34	0.0007	
X <sub>3</sub> X <sub>1</sub>	42.87	1	42.87	23.37	0.0162	
Residuals	18.47	10	1.83			
Lack-of fit	14.03	5	2.81	3.25	0.1107	Not significant
Pure error	4.31	5	0.86			

implied that the model was significant. Value of Prob> F less than 0.05 also indicated that the model terms were significant. In this case, X<sub>1</sub>, X<sub>2</sub>, X<sub>3</sub>, X<sub>1</sub><sup>2</sup>, X<sub>2</sub><sup>2</sup>, X<sub>3</sub><sup>2</sup> and interaction terms of X<sub>1</sub>X<sub>2</sub>, X<sub>1</sub>X<sub>3</sub>, and X<sub>2</sub>X<sub>3</sub> were significant model terms.

However, the statistical results obtained here showed that the aforementioned two models were adequate to predict the yield and removal percentage of manganese within the range of variables studied here to prepare activated carbon.

CV value indicates the ratio between standard error of estimate with the mean value of the observed response as percentage. It measures the reproducibility of the model and if it is less than 10% then the model can be considered reasonably reproducible. It was found that the CV values obtained for yield and percentage removal

were 5.68 and 1.67 showing reproducibility of the models.

#### Lack-of-fit test

The discrepancies between measured and expected values can be attributed to systematic error. That is the reason lack of fit test is used to compare between residual error with pure error from replicated design points (Azargohar and Dalai, 2005). However, in this present study, for carbon yield and percentage removal of manganese, the probability>F values are representing not significant lack of fit which is desirable. In this research, for carbon yield and percentage removal; probability > F values obtained were 0.3875 and 0.1107; respectively representing lack of fit is not significant relative to pure error.

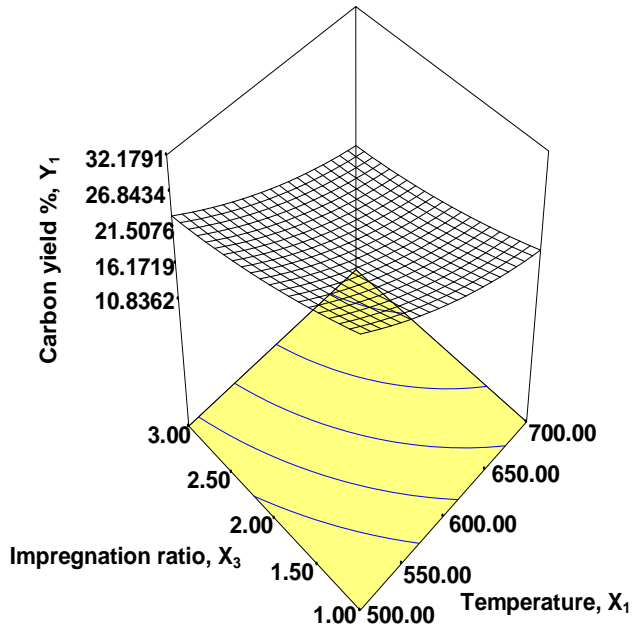


**Figure 2.** Effect of activation temperature and chemical impregnation ratio on percentage yield: 3D surface graph and contour plot.

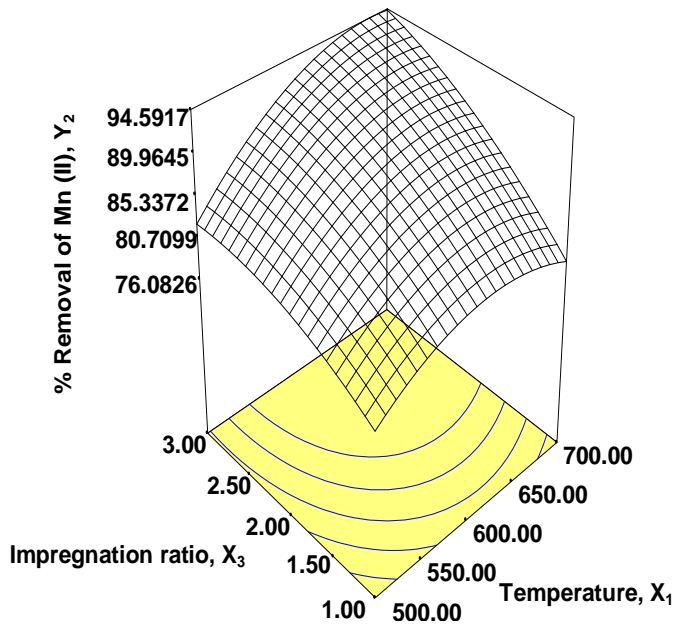


**Figure 3.** Effect of activation temperature and chemical impregnation ratio on percentage Removal; 3D surface graph and contour plot.

### Effect of preparation variables

The graphical representations of the developed models based on Equations (10) and (11) are shown by 3D surface graphs and contour plots by Figures 2 and 3. These figures illustrate the effects of different variables

and their interactions on the responses of percentage yield and percentage removal of manganese from water sample.

Figure 2 shows the three dimensional response surfaces, the combined effect of activation temperature and impregnation ratio for yield at constant time of 2 h. The carbon yield was found to decrease with increasing temperature, time and impregnation ratio. The highest yield of 34.99% was achieved when all the three preparation variables were at the minimum point within the range studied. Among all three variables studied here, temperature was found to have greatest effect than activation time and impregnation ratio. Similar results were also observed by previous researchers for preparation of activated carbon from oil palm fiber and rattan sawdust (Hameed et al., 2008; Ahmad et al., 2009). Increasing temperature will simultaneously increase evolution of volatile matter and carbon burn off leading to dehydration. On the other hand, elimination reactions between the precursors and the activating agents like KOH and CO<sub>2</sub> results in more porous structure and less yield than the lower temperature (Adinata et al., 2007).

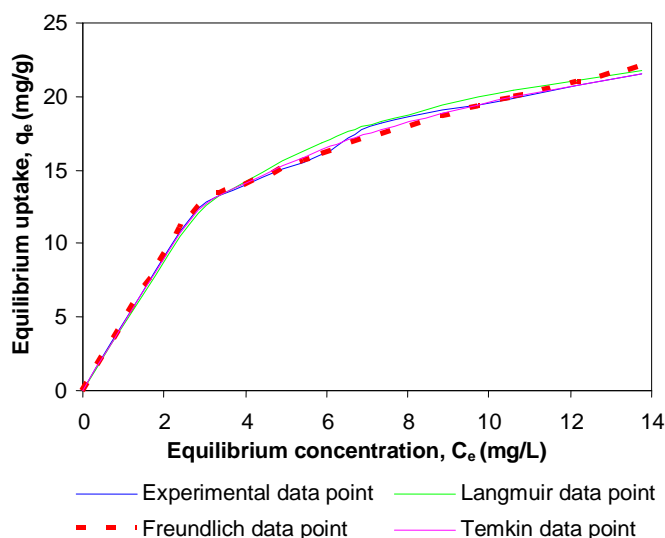
Figure 3 shows that the removal percentage increased with the increase of activation temperature and impregnation ratio. The curvature obtained in Figure 3 represents that the interactions between activation temperature and impregnation ratio on removal percentage was pronounced and it was further confirmed by significance test. It was found by previous researchers also that, the activation time had least impact on the development of pore structure of the activated carbon prepared from cassava peel and the pore characteristics were influenced strongly by KOH impregnation ratio and temperature (Sudaryanto et al., 2006). This observation was in agreement with the previous research carried out by physical activation of apricot stone, physio-chemical activation of oil palm fronds and chemical activation of tamarind wood for production of activated carbon (Sentorun-Shalahy et al., 2006; Salman and Hameed, 2010; Sahu et al., 2010). The highest removal percentage of 91.09% was observed at the axial points of 600°C temperature, time 2 h and impregnation ratio, IR of 3.68. Most probably at higher temperature of 700 or 768.18°C and activation time more than 2 h had produced activated carbon with less surface area due to destruction of pore structure, surface functional groups and high ash content which could not retain small cations like manganese. Similar observation was reported for preparation of activated carbon from oil palm empty fruit bunches for removal of zinc (Zahangir et al., 2008). However, the three preparation variables studied here have synergistic effects on absorption capacity of Mn(II) ions from synthetic waste water.

### Process optimization

The function of desirability with preparation conditions

**Table 7.** Isotherm model parameters and correlation coefficient at 30°C temperature.

Isotherm model	Parameter	Value	R <sup>2</sup>
Langmuir	q <sub>m</sub> , maximum monolayer adsorption capacities(mg/g)	27.78	0.997
	R <sub>L</sub> , separation factor	0.04	
	K <sub>L</sub> , Langmuir constant	0.2628	
Freundlich	K <sub>F</sub> , Affinity factor (mg/g(l/mg) <sup>1/n</sup> )	8.3645	0.990
	1/n, Freundlich exponent	0.368	
Temkin	B(J/mol), Temkin constant	5.997	0.994
	K <sub>T</sub> (l/g), Binding constant	2.627	

**Figure 4.** Relation between  $C_e$  and  $q_e$  for Mn (II) removal on activated carbon prepared at optimum condition at 30°C temperature.

was applied. Based on economical perspective of production process, the variables were set within the studied range and goals were targeted to achieve maximum possible yield with removal percentage by the software. The optimum condition chosen by the software was: activation temperature, activation time and impregnation ratio of 574°C, 1.31 h and IR 3, respectively to obtain highest removal efficiency and yield. At this optimum condition, activated carbon was prepared and the carbon yield and removal percentage obtained were 20.61 and 88.14%. The experimental values obtained were in good agreement with the predicted results by the software with relatively small errors of 2.71 and 2.16%, respectively.

### Adsorption isotherm

The use of adsorption isotherm depicts the relationship

between  $C_e$  and  $q_e$  at equilibrium contact time. The model parameters are listed in Table 7. The actual experimental data points along with other isotherms are plotted in Figure 4. The plot resulted with almost L-shaped curve which shows high affinity between adsorbate and adsorbent (Datchaneekul, 2005). The validity of the Langmuir model here, recommended that the adsorption process was monolayer (Pruksathorn and Vitidsant, 2009; Chowdhury et al., 2011 b, c) and adsorption of each molecule had equal activation energy. The  $R_L$  value obtained was less than 1 indicating that the adsorption of Mn (II) onto the prepared activated carbon is favorable. The Langmuir model was found to fit the data significantly better than Freundlich model, which showed the more homogeneous nature of the activated carbon. The positive value of  $K_F$  also reflects strong adsorbate-adsorbent interactions. Freundlich exponent,  $1/n$  ranging between 0 and 1 is a measure of adsorption surface heterogeneity. The value  $1/n$  below one reflects favorable



**Table 8.** Physio-chemical characteristics of activated carbon.

Physio-chemical characteristics	Value
BET surface area	386.03 m <sup>2</sup> /g
Langmuir surface area	702.4 m <sup>2</sup> /g
Micropore surface area	278.6 m <sup>2</sup> /g
Total pore volume	0.233 cm <sup>3</sup> /g
Average pore diameter	2.41° A
Cumulative adsorption surface area (BJH method)	219.8 m <sup>2</sup> /g
t- method for micro- pore surface area	278.6 m <sup>2</sup> /g
Bulk density	0.323 g/ml

adsorption of Mn (II) onto the surface of prepared activated carbon. The experimental data were further analyzed by Temkin isotherm which showed a higher regression coefficient,  $R^2$  of 0.994, enlightening the linear dependence of heat of adsorption at low or medium coverage.

### Characterization of the optimally prepared activated carbon

#### BET surface area and pore volume

The surface area and pore size distribution plays a vital role for adsorption process. The BET surface area and total pore volumes increased significantly as the activation process used both chemical and physical activating agents of KOH and CO<sub>2</sub>. However, semi carbonization step was important as it can increase the diffusion of KOH and CO<sub>2</sub> molecules into the pores and thereby enhance the BET surface area and volume of the pore. According to the IUPAC classification, the average pore diameter of 2.41° A represents that the prepared activated carbon is of mesoporous type (IUPAC Terminology 1972). The physio-chemical characteristics of the prepared activated carbon are listed in Table 8.

#### Surface morphology

Figures 5a to c, show the SEM images of the precursor semi carbonized sample and the final activated carbon obtained under the optimum preparation conditions, respectively. As can be seen from Figure 5a, there is few pores available on the surface of the precursor. Figure 5b shows rough texture of the fiber with the presence of irregular shaped pores after semi carbonization stage. Figure 5c shows that the physiochemical activation process by using KOH and CO<sub>2</sub> was effective in creating well-developed pores on the surfaces. Similar observations were reported by the previous researchers for preparation of activated carbons from pistachio-nut shells (Lua and Yang, 2004).

### Surface chemistry

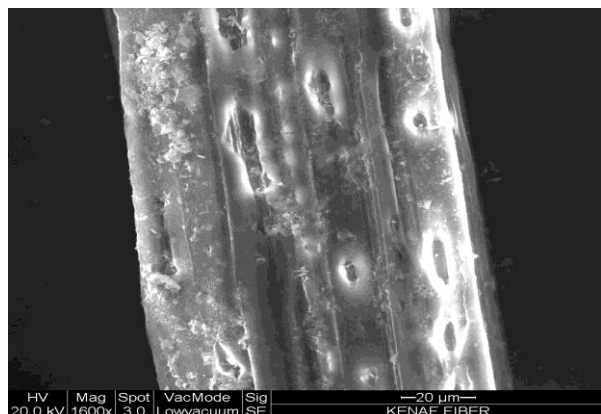
FTIR spectrum is useful to identify the surface functional groups which can contribute significantly to enhance absorption efficiency. Figure 6 and Table 9 show that the surface chemistry of the activated carbon is different from the precursors as many of the functional groups shifted or disappeared after carbonization and activation processes due to thermal degradation effect during the carbonization and activation process. Some new peaks were also detected in semicarbonized sample. These changes in the spectrum clearly indicates the possible involvement of KOH and CO<sub>2</sub> to amend the surface chemistry of the prepared activated carbon than the raw precursor. Previous studies based on activated carbon prepared from rice straw (Oh et al., 2003) and cherry stone (Olivares- Marn et al., 2006) also reported the presence of same types of surface functional groups.

### Elemental analysis

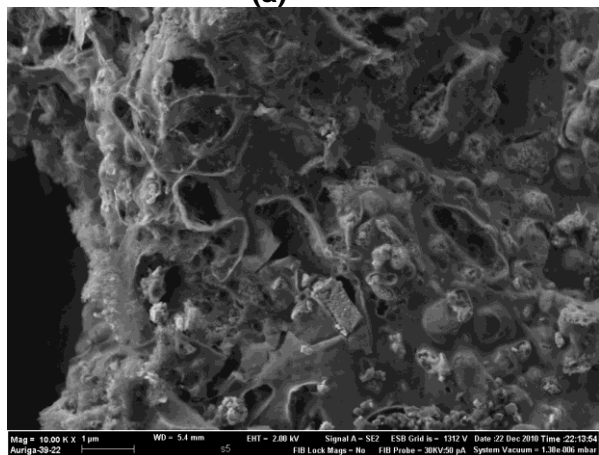
The elemental analysis of the precursor and activated carbon prepared under the optimum condition indicated that the percentage of C, H, N and others found in the precursor, semi carbonized sample and activated carbon were 42.85, 5.33, 0.33 and 51.49% for precursor and 47.26, 7.34, 0.34 and 44.98% for semi carbonized fiber and 69.91, 3.29, 0.80 and 26.0% for activated carbon. All the samples have moderate nitrogen content. It was observed that the carbon content increased significantly after activation of the raw fiber revealing that physiochemical activation method was suitable to develop activated carbon from kenaf fiber which can subsequently enhance the uptake capacity of Mn (II) from contaminated water.

### Conclusion

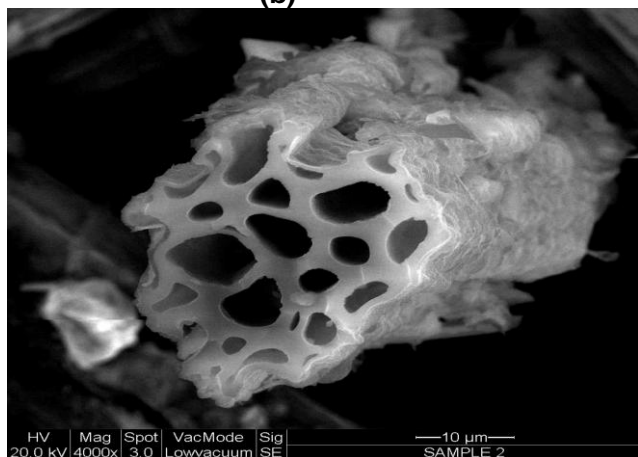
In this research, quadratic models were developed to correlate the effect of preparation variables with the responses of percentage yield and removal of Mn (II) ions



(a)



(b)



(c)

**Figure 5.** Scanning electron micrograph: (a) Raw Kenaf fiber, (b) semi carbonized sample and (c) activated carbon.

from synthetic waste water by using kenaf fiber based activated carbon. Activation temperature and impregnation ratio played the most significant role for both the responses. Process optimization was carried out and it was found that the experimental results agreed satisfactorily with the predicted result by the model. It

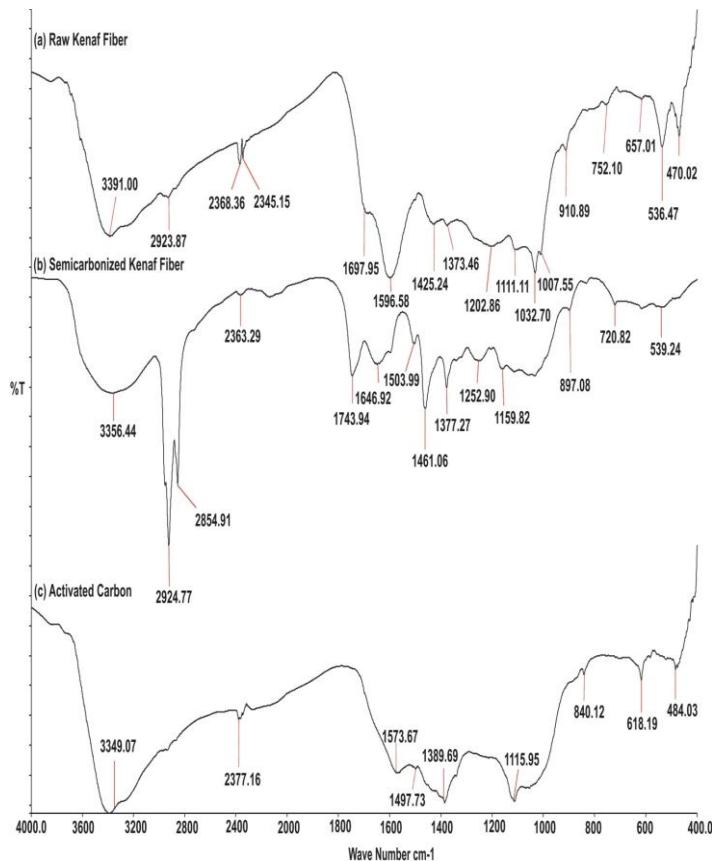


**Figure 6.** FTIR spectra: (a) Raw Kenaf fiber; (b) Semi carbonized sample and (c) Activated carbon.

was observed that the activation technique was successful to prepare activated carbon from kenaf fiber. The prepared carbon showed some unique features of surface area, pore size distribution and surface functional groups which played significant role to absorb Mn (II) ions from aqueous sample. The equilibrium data were well represented by the Langmuir isotherm, giving maximum monolayer adsorption capacity as high as 27.78 mg/g at 30°C. For commercial production of activated carbon to be used on industrial scale, sufficient yield, high removal efficiency along with abundant availability of the precursor is essential. By considering the aforementioned point, it can be concluded that, activated carbon prepared from kenaf fiber is economically viable, environmentally friendly and promising material which can be used successfully for separation of Mn (II) from contaminated water.

## ACKNOWLEDGEMENTS

The authors are grateful for the financial support of this project by Research Grant (UMRG 056-09SUS) and Bright Spark Unit of University Malaya, Kuala Lumpur 50603, Malaysia.

**Table 9.** Analysis of FTIR spectra.

IR Peak	Frequency (cm <sup>-1</sup> )			Assignment
	Raw Kenaf fiber	Semi carbonized Kenaf fiber	Activated Kenaf fiber	
1	470.02	-	484.03	C-H out-of-plane bending of benzene derivatives
2	536.47	539.24	-	C-H bending
3	657.01	-	618.19	C-O-H
4	752.10	720.82	-	C-H out-of-plane bending of benzene derivatives
5	-	897.08	840.12	C-H out-of-plane bending of benzene derivatives
6	910.89	-	-	O-H bending
7	1007.55	-	-	C-O-C stretching of esters, ethyl or phenyl group
8	1032.70	-	-	C-O-C stretching of esters, ethyl or phenyl group
9	1111.11	1159.82	1115.95	-C-N stretching
10	1202.86	1252.90	-	C-O stretching
11	1373.46	-	1389.69	CH <sub>3</sub> deformation
12	-	1327.27	-	-NO <sub>2</sub> aromatic nitro compound
13	1425.24	1461.06	1497.73	in-plane OH bending and C-O stretch of dimmers
14	1596.58	1503.99	1573.67	C=C ring stretching of benzene derivatives
15	1667.95	1646.92	-	C=O stretching
16	-	1743.94	-	C=O stretching
17	2345.15	-	-	C=C stretching vibration of ketones, aldehydes or carboxylic group
18	2368.36	2363.29	2377.16	C=C stretching vibration of ketones, aldehydes or carboxylic group
19	-	2854.91	-	C-H stretching
20	2923.87	2924.77	-	C-H stretching
21	3391.00	3356.44	3349.07	O-H stretching vibration of hydroxyl functional groups

**Abbreviations:** **KF**, Kenaf fiber; **ANOVA**, analysis of variance; **CV**, coefficient of variation; **RSM**, response surface methodology; **CCD**, central composite design; **q<sub>max</sub>(mg/g)**, Langmuir maximum monolayer adsorption capacity; **q<sub>e</sub>(mg/g)**, equilibrium uptake; **K<sub>L</sub>(l/mg)**, Langmuir constant; **R<sub>L</sub>**, separation factor; **C<sub>e</sub> (mg/L)**, equilibrium concentration; **C<sub>0</sub> (mg/L)**, Initial concentration; **K<sub>F</sub> (mg/g(l/mg)<sup>1/n</sup>)**, Freundlich constant or affinity factor; **1/n**, heterogeneity factor or Freundlich exponent; **B(J/mol)**, Temkin constant; **K<sub>T</sub> (l/g)**, equilibrium binding Constant.

## REFERENCES

- Aber S, Khataee A, Sheydaei M (2009). Optimization of activated carbon fiber preparation from Kenaf K<sub>2</sub>HPO<sub>4</sub> as chemical activator for adsorption of phenolic compounds. *Bioresour. Technol.*, 100: 586-6591.
- Adinata D, Daud MAW, Aroua MK (2007). Preparation and characterization of activated carbon from palm shell by chemical activation with K<sub>2</sub>CO<sub>3</sub>. *Bioresour. Technol.*, 98: 145-149.
- Ahmad AA, Hameed BH (2010). Effect of preparation conditions of activated carbon from Bamboo Waste for Real Textile wastewater. *J. Hazard. Mater.*, 173: 487-493.
- Ahmad AA, B.H. Hameed BH, Ahmad AL (2009). Removal of disperse dye from aqueous solution using waste-derived activated carbon: Optimization study. *J. Hazard. Mater.*, 170: 612-619.
- Akpor OB, Muchie M (2010). Remediation of heavy metals in drinking water and waste water treatment systems: Processes and applications. *IJPS*. 5(12): 1807-1817.
- Azargohar R, Dalai AK (2005). Production of activated carbon from Luscarchar: experimental and Modelling studies. *Micropor. Mesopor. Mater.*, 85: 219-225.
- Baquero MC, Giraldo L, Moreno JC, Suarez-Garcia F, Martinez-Alonso A, Tascon JMD (2003). Activated carbons by pyrolysis of coffee bean husks in presence of phosphoric acid. *J. Anal. Appl. Pyrol.*, 70: 779-784.
- Chowdhury ZZ, Zain SM, Rashid AK, Khalid K (2011a). Linear regression analysis for Kinetics and Isotherm studies of sorption of Manganese (II) ions onto activated palm ash from waste water. *Orientchem.*, 27(2): 405-415.
- Chowdhury ZZ, Zain SM, Rashid AK, Ahmed AA (2011b). Equilibrium Kinetics and Isotherm Studies of Cu (II) Adsorption from Waste Water onto Alkali Activated Oil Palm Ash. *Am. J. Appl. Sci.*, 8(3): 230-237.
- Chowdhury ZZ, Zain SM, Rashid AK (2011c). Equilibrium Isotherm Modelling, Kinetics and Thermodynamics Study for removal of lead from waste water. *E. J. Chem.*, 8(1): 333-339.
- Datchaneekul K (2005). Removal of Heavy metals in synthetic waste water by Adsorption on Bentonite. M.Sc. dissertation, Mahidol University, Bangkok, Thailand.
- Diao Y, Walawender WP, Fan LT (2002). Activated carbons prepared from phosphoric acid activation of grain sorghum. *Bioresour. Technol.*, 81: 45-52.
- Do DD (1996). A Model for Surface Diffusion of Ethane and Propane in Activated Carbon. *Chem. Eng. Sci.*, 51(17): 4145-4158.
- Egila JN, Dauda BEN, Iyaka YA, Jimoh T (2011). Agricultural waste as low cost adsorbent for metal removal from waste water. *IJPS*. 6(8): 2152-2157.
- Freundlich HMF (1906). Over the adsorption in solution. *J. Phys. Chem.*, 57: 385-470.
- Gomez-Serrano V, Cuerda-Corra EM, Fernandez-Gonzales MC, Alexandre-Franco MF, Macias Garcia A. (2005). Preparation of activated carbons from chestnut wood by phosphoric acid chemical

- activation, study of microporosity and fractal dimension. *Mater. Lett.*, 59: 846-853.
- Gratuito MKB, T. Panyathanmaporn T, Chumnanklang RA, Sirinuntawittaya NB, Dutta A (2008). Production of activated carbon from coconut shell: optimization using response surface Methodology. *Bioresour. Technol.*, 99: 4887-4895.
- Hameed BH, Tan IAW, Ahmad AL (2008). Optimization of basic dye removal by oil Palm fibre- based Activated carbon using response surface methodology. *J. Hazard. Mater.*, 158: 324-332.
- Hefne JA, Mekhemer WK, Alandis NM, Aldayel OA, Alajyan T (2008). Kinetics and thermodynamic study of the adsorption of Pb (II) from aqueous solution to the natural and treated Bentonite. *IJPS.* (11): 281-288.
- Hu Z, Srinivasan MP (1999). Preparation of high-surface-area activated carbons from coconut shell. *Micropor. Mesopor. Mater.*, 27: 11-18.
- IUPAC (1972). IUPAC manual of symbols and terminology, *Pure Appl. Chem.*, 31: 587.
- Ismadji S, Bhatia SK (2001). Characterization of activated carbons using liquid phase adsorption. *Carbon*, 39: 1237-1250.
- Karacan F, Ozden U, Karacan S (2007). Optimization of manufacturing conditions for Activated Carbon from Turkish lignite by chemical activation using response surface Methodology. *Appl. Therm Eng.*, 27: 1212-1218.
- Langmuir I (1916). Constitution and fundamental properties of solids and liquids. I. Solids. *J. Am. Chem. Soc.*, 38(11): 2221.
- Lee J, Ye L, Landen WO, Eitenmillcr RR (2000). Optimization of an extraction procedure, for the quantification of vitamin E in tomato and broccoli using respons surface methodology. *J. Food Compos. Anal.*, 13: 45-57.
- Lua AC, Yang T (2004). Effect of activation temperature on the textural and chemical properties of potassium hydroxide activated carbon prepared from pistachionut shell. *J. Colloid Interface Sci.*, 274: 594-601.
- Mattson JS, Mark HB (1971). *Active Carbon*, MarccI Dekker, INC. New York, pp. 1-5.
- Oh GH, Yun CH, Park CR (2003). Role of KOH in the one-stage KOH activation of Cellulosic Biomass. *Carbon Sci.*, 4(4): 180-184.
- Olivares-Marn M, Fernandez-Gonzalcz C, Macras-Garcia A, Gomez-Serrano V (2006). Preparation of activated carbons from cherry stones by activation with potassium hydroxide. *Appl. Surf. Sci.*, 252: 5980-5983.
- Parajo JC, Alonso JL, Lage MA, Vazquez D (1992). Empirical Modeling of *Eucalyptus* Wood Processing. *Bioprocess Eng.*, 8: 129-136.
- Prahas D, Kartika Y, Indraswati N, Ismadji S (2008). Activated carbon from jackfruit peel waste by H<sub>3</sub>PO<sub>4</sub> chemical activation: pore structure and surface chemistry characterization. *Chem. Eng. J.*, 140: 32-42.
- Pruksathorn P, Vitidsant T (2009). Production of Pure Ethanol from Azeotropic Solution by Pressure Swing Adsorption. *Am. J. Eng. Appl Sci.*, 2(1): 1-7.
- Puziy AM, Poddubnaya OI, Martnez-Alonso A, Suarez-Garcia F, Tascon JMD (2005). Surface Chemistry of phosphorus-containing carbons of lignocellulosic origin. *Carbon*, 43: 2857-2868.
- Sahu JNJ, Acharya J, Meikap BC (2010). Optimization of production conditions for activated Carbons from *Tamarind wood* by zinc chloride using response surface methodology. *Bioresour. Technol.*, 101: 1974-1982.
- Salman JM, Hameed BH (2010). Effect of preparation conditions of oil palm fronds Activated Carbon on adsorption of bentazon from aqueous solutions. *J. Hazard. Mater.*, 175: 133-137.
- Sayan E (2006). Ultrasound-assisted preparation of activated carbon from alkaline impregnated hazelnut shell: An optimization, study on removal of Cu<sup>2+</sup> from Aqueous Solution. *Chem. Eng. J.*, 115: 213-218.
- Sentorun-Shalahy C, Ucak-Astarlioglu MG, Artok L, Sarici C (2006). Preparation and characterization of activated carbons by one-step steam pyrolysis/activation from apricot Stones. *Micropor. Mesopor. Mater.*, 88: 126-134.
- Srinivasakannan C, Bakar MZA (2004). Production of activated carbon from rubber wood Sawdust. *Biomass Bioenergy* 27: 89-96.
- Stavropoulos GG, Zabaniotou AA (2005). Production and characterization of Activated Carbons from olive-seed waste residue. *Micropor. Mesopor. Mater.*, 83: 79-85.
- Sudaryanto Y, Hartono SB, Irawaty W, Hindarso H, Ismadji S (2006). High surface area Activated Carbon prepared from cassava peel by chemical activation. *Bioresour. Technol.*, 97: 734-739.
- Tan IAW, Ahmad AL, Hameed BH (2008). Preparation of activated carbon from coconut husk: Optimization on Removal of 2, 4, 6 Trichlorophenol using response surface methodology, 153: 709-717.
- Tay JH, Chen XG, Jeyaseelan S, Graham N (2001). Optimising the preparation of Activated Carbon from digested sewage sludge and coconut husk. *Chemosphere*, 44: 45-51.
- Temkin MI, Pyzhev V (1940). Kinetics of Ammonia synthesis on promoted iron catalyst. *Acta Physicochemica. USSR*, 12: 327-356.
- Zahangir MA, Suleyman AM, Noraini K (2008). Production of activated carbon from oil Palm empty fruit bunches for removal of zinc. Twelfth International Water Technology Conference, (IWTC12), Alexandria, Egypt, pp. 373-383.
- Zainudin NF, Lee KT, Kamaruddin KT, Bhatia S, Mohamed AR (2005). Study of Adsorbent prepared from oil palm ash (OPA) for flue gas desulfurization. *Sep. Purif. Technol.*, 45: 50-60.